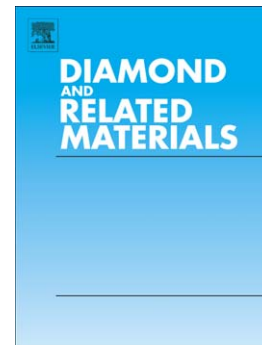# Accepted Manuscript

Thermal Stability in Oxidative and Protective Environments of a-C:H Cap Layer on a Functional Gradient Coating

C. Louro, C. Wagner Moura, N. Carvalho, M. Stueber, A. Cavaleiro

Please cite this article as: C. Louro, C. Wagner Moura, N. Carvalho, M. Stueber, A. Cavaleiro, Thermal Stability in Oxidative and Protective Environments of a-C:H Cap Layer on a Functional Gradient Coating, *Diamond & Related Materials* (2010), doi: 10.1016/j.diamond.2010.11.010

Thermal Stability in Oxidative and Protective Environments of a-C:H Cap Layer on a Functional Gradient Coating

C. Louro[1*], C. Wagner Moura[2], N. Carvalho[3], M. Stueber[4], A. Cavaleiro[1]

[1] SEG-CEMUC, Departamento de Engenharia Mecânica, Universidade de Coimbra, Polo II , Rua Luis Reis, 3030-788 Coimbra, Portugal.

[2] REDEMAT - Laboratório de Engenharia e Modificações de Superfícies, Av. José Cândido da Silveira, 2000, Horto, 31.170-000, Belo Horizonte, Minas Gerais, Brasil.

[3] NV Bekaert SA, Bekaertstraat 2, 8550 Zwevegem, Belgium.

[4] Forschungszentrum Karlsruhe, Institute of Materials Research I, Hermann-von-Helmholtz-Platz 1, D-76344 Eggenstein-Leopoldshafen, Germany.

* **Corresponding author**: SEG-CEMUC, Departamento de Engenharia Mecânica, Universidade de Coimbra, Polo II, Rua Luís Reis, 3030-788 Coimbra, Portugal. Tel./Fax: +351239790700/+351 239790701, E-mail address: cristina.louro@dem.uc.pt

Abstract

Three types of hydrogenated amorphous carbon (a-C:H) coatings were synthesized on stainless steel substrates by a Plasma Assisted CVD process, containing hydrogen contents in the range from 25 to 29 at.%. The effect of annealing up to 600 ºC in two different environments on both the structure and the mechanical properties of the coatings was investigated by means of Differential Scanning Calorimetry/Thermogravimetry (DCS/TG), Raman Spectroscopy and Depth Sensing Indentation. The results indicate that the structural modifications occurred in the coatings in both protective and oxidative atmospheres up to 400ºC were due to a complex atomic rearrangement involving the dehydrogenation reaction. A small weight loss, detected by isothermal TG analysis confirmed the H_2 effusion. This dense effect proceeds without a change of hardness which was maintained in the diamond-like regime. The annealing in non-oxidative ambiance at temperatures above 500ºC causes both gaseous products effusion and sp^3 to sp^2 transformation. Raman parameters and hardness values were, under these conditions, similar to those known for a typical graphite-like regime. While the onset temperature of the graphitization process was found to be almost independent of the H content range investigated, the situation was completely different in

relation to the oxidation reaction. The highest oxidation resistance was found for coatings with the lowest H content.

1. Introduction

Literature on diamond-like carbon (DLC) films has become very extensive and widespread in the past decades. The combination of physical, chemical and mechanical properties, similar to diamond but without a crystalline lattice structure, together with the relatively easy to synthesize and lower cost of preparation, makes DLC a strong candidate as a surface engineering material. Nevertheless, and in spite of their popularity, DLC coatings present some basic disadvantages limiting their fully application in exploitation tribological contacts.

One of the main drawbacks reported in literature is their low thermal stability. As the temperature is increased, the structure of DLC films, which is claimed to be a metastable form of carbon with mixture of sp^3/sp^2 bonds [1, 2], collapses into a more sp^2-bonded network by a sp^3 diamond-like domains conversion. This instability, denominated as *graphitization* process, is extremely noticeable in the one of the major DLC family, the H-containing form of amorphous carbon (a-C:H) [3-11]. It is well known that hydrogen stabilizes the diamond structure by maintaining the sp^3 hybridization configuration. However, when the coatings are exposed to heat treatments in vacuum or in air, the effusion of hydrogen occurs. Concomitantly to thermal decomposition of a-C:H films into gaseous products, such as H_2 and hydrocarbon C_xH_y, in particular CH_4 and C_2H_6 [12-14], the conversion of sp^3 to sp^2 bonds and the consequent loss of diamond-like properties have been observed. Typically for a-C:H coatings, the graphitization onset temperature ranges from 250 to 500 ºC depending on the deposition and growth process [3-11]. Therefore, the study of the irreversible changes on the a-C:H coatings structure by annealing is an important issue for practical coatings applications.

In the present work, the thermal stability up to 600ºC of commercially available a-C:H films was studied. In order to improve adhesion to substrate, another drawback of these materials, a functionally gradient type of coatings was deposited by Plasma Assisted Chemical Vapour Deposition (PACVD). Besides external hydrogenated amorphous carbon top layer, two

intermediate layers (a Ti layer adjacent to the substrate followed by a Si containing transition layer) were sequentially deposited on stainless steel substrates. The thermal behaviour of the films, prepared under similar conditions but with different precursor gases, is compared by selecting two different environments in the same temperature range. The motivation of the work is to describe the individual thermally induced effects and their interrelation, by annealing the coatings in a non-oxidative environment and under real conditions of most practical importance for tribological applications, which will be attained by heat treatments in air.

2. Experimental procedure

Patented DLC-based coatings [15] were deposited by NV Bekaert SA Company onto stainless steel substrates (AISI 310) by PACVD process using an industrial scale R&D reactor (1370x1370x1522mm). Three different precursors gases were used with a H/C ratio between 1 and 4 in order to achieve H contents up to 30 at.%. A compound interface consisting of a Ti interlayer and a Si containing transition layer were deposited sequentially before the final deposition of the a-C:H top layer. Due to the rotation of the substrate holder, all the faces of the steel samples (5x5x1 mm) were uniformly coated.

The hydrogen concentration was determined by Elastic Recoil Detection Analysis, TOF-ERD, using a ^{63}Cu beam operating at 12 MeV. Thermogravimetric (TG) and Differential Scanning Calorimetric (DSC) analyses were carried out in a Polymer Science Thermobalance STA-1500 of high-resolution (0.1 μg) up to 800 ºC. The coatings were characterized in two different environments: non-oxidative (Ar-5%H_2) and oxidative (N_2-20%O_2) introduced in the thermobalance at a flow rate of 55 sccm. Isothermal annealing temperatures ranged from 250 to 600 ºC and were held for 60 min.

Several analytical techniques were used in this study to characterize the effect of annealing on the coatings. The identification of sp^3/sp^2 bond conversion was investigated by Raman Spectrometry using a Renishaw system 1000 at a wavelength of 514.5 nm at 50 mW Ar^+ ion laser power. The Raman spectra obtained were deconvoluted in the D and the G bands by curve fitting using Gaussian lines. The morphological characteristics and the thickness variation of the annealed

coatings were established by cross-section observation in a Philips-SEM operated at 20 kV. The structural evolution was investigated by X-ray diffraction (XRD) in Bragg-Brentano configuration with a Philips X-Pert diffractometer (Co-K_α radiation).

Mechanical properties were evaluated by Ultramicroindentation in a Fisherscope H100 apparatus. The results obtained are an average of 10 indentations performed under the applied load of 20 mN. The hardness values were corrected for the geometrical imperfections of the Vickers indenter, the thermal drift of the equipment, and the uncertainty in the zero position following the method proposed by Antunes *et al*. [16].

3. Results and discussion

3.1. As-deposited coatings

The fundamental characteristics of the three series of DLC-based coatings are presented in table 1. By changing the H/C ratio of the precursor gases used for deposition, the analyses made by TOF-ERD revealed that the H-content in the external layer ranged from 25 to 29 at.%. Besides C and H only vestiges of O (< 0.2 at.%) and Ar were detected in the films. The use of argon as a carrier gas for some of the precursors gave rise to its incorporation during film formation with contents of up to 1.2 at. % (table 1). The coatings are chemically homogeneous with no significant variation of the composition, as is demonstrated by ERD elemental composition in figure 1a) for the as-deposited Film *1*.

Considering the structural bonding of the as-deposited coatings, figure 1b), all the films are characterized by two broad peaks centred at 1530-1570 cm^{-1} and 1350 cm^{-1}, which are denoted as G and D bands, respectively [1, 2]. According to some authors [1, 4, 17], the main effect of H in an a-C:H film is to modify the C-C bonding, not by increasing their fraction but terminating the sites of double bonding of carbon as $C(sp^3)$-H_x (x= 1,2,3) giving rise to higher sp^3 contents in the film. Hence, with increasing H content, a drop in the extents of double bonds occurs and consequently the hardness of the coating decreases. The use of a recent empirical relation [18], based on Raman measurements, allows to correlate the hardness as a function of the hydrogen content in a-C:H films by,

$$hardness[GPa] = 44.195 - 0.93 \times (\%at.H) \qquad (1)$$

Applying the equation (1) to the coatings in study, the hardness values vary from 17 to 21 GPa, which are in general good agreement with the experimental ones (see table 1), although, for the latter ones, the trend is opposite, i.e., the hardness drops with decreasing H content. It is important to point out that the equation authors [18] apply to Raman analysis based on the G-band position only (after fitting procedure with six Lorentzians and a linear background) and thus the reason for the observed mismatch. Analyzing the Raman spectra, figure 1b), no significant variations can be observed among the as-deposited films. However, the peak fitting of experimental data (see the deconvoluted Gaussian lines for Film *3* insert in figure 1b)) allows the detection of a small increase of the D/G peak ratio and a shift of the G band position to higher frequencies with decreasing H content. These evolutions suggest a tendency for a more graphitic structure. The measured mechanical properties (table 1) are kept in the diamond-like regime with Young's modulus ($\cong 160$ GPa) and hardness values ($\cong 20$ GPa) typical of hard a-C:H films containing 10-40 at.% H in opposition to soft or polymeric a-C:H which present high hydrogen content ($40 <$ at.% H < 65) and lower hardness values (< 5 GPa) [19, 20].

In respect to the as-deposited morphology, the cross-section SEM micrograph of the coating with 27 at.% H shown in figure 1a) present a continuous and smooth defect-free external a-C:H layer typical of featureless type morphologies. The surface roughness values are very low, with Ra values less than 10 nm in all films.

3.2. Annealing Experiments

3.2.1. Oxidative Environment

a-C:H films were detached from the substrates and the resulting powders were examined by DSC/TG in continuous heating in air ambiance with a heating rate of 20 °C.min^{-1} up to 800 °C. An example of the thermal analysis curve is shown in figure 2a) for Film *3*. As can be observed, the DSC signal revealed a well defined exothermal reaction which could be associated to the oxidation of carbon according to the reaction (2) proposed in literature [21, 22],

$$C_{(s)} + O_{2(g)} \rightarrow CO_{2(g)} \tag{2}$$

The TG signal is in agreement with the formation of gaseous oxidation products by showing a significant weight loss, 89 %, between 525 and 605 ºC. Based on these results, isothermal TG tests were performed at four different temperatures with films deposited on the SS (AISI 310) substrates. The weight variation (Δm/Area) obtained after heat exposure for 60 min are shown in figure 2 (b to d). The analysis of these evolutions allows us to conclude that independently of the H-content the mass loss is as greater as the oxidation temperature is. Below 400 ºC, all coatings maintain their integrity with no significant weight variation during the entire isothermal time duration. At 500 ºC the oxidation of carbon starts to take place with the consequent increasing weight loss with testing time.

The outward diffusion of the gaseous compounds formed by oxidation and/or dehydrogenation processes, as was anticipated by DSC tests, become more and more evident at 600 ºC, particularly for the highest H-content film. At this temperature the resistance to oxidation is very low. In these films, the tendency for weight stabilization after 60 min annealing in air suggests that the external a-C:H layer is almost consumed, being now the behaviour determined by the adhesion graded transition layers. However, in opposition to others research works on oxidation behaviour of DLC-type coatings [21, 22], the highest temperature used in this study was not enough to promote visible oxidation of the underlying layers and the steel substrate. In fact, XRD patterns did not reveal any oxide phases, as can be confirmed in figure 3 for Film *3*. Up to 500 ºC only XRD peaks related to the SS310 substrate and to the Ti/Si interlayer could be detected. At 600 ºC, the new diffraction lines could be indexed as belonging to TiC, SiC or Ti_5Si_3 phases, indicating that some thermal bulk diffusion are enhanced, but never to any type of oxide phase. The formation of stable inter-diffusion phases at the substrate-coating interface, by selecting both Ti and Si for the gradient transition composition, provides good results by avoiding the substrate oxidation. These results outstand those obtained by Wang *et al.* [21] who reports the oxidation of the underlying TiN/TiC_xN_y functional gradient layer, for temperatures as low as 450 ºC, in addition to a-C:H external layer oxidation.

TG results are in good agreement with the coating thickness measured by SEM cross-section after each isothermal annealing. Figure 4 plots the normalized thickness variation of the external a-C:H layer in relation to the as-deposited value, as a function of the oxidation temperature. Again, the superior resistance of Film *1* in relation to Film *2* and *3* can be stated by the maximum loss of about 50 % at 600 ºC, whereas the a-C:H external layer of both Film *2* and *3* completely disappeared at this temperature. Moreover, for these two last coatings the trend is much steeper which confirmed their lower oxidation resistance in relation to Film *1* in addition to good uniform and homogenous adhesion. The surface morphology of the external a-C:H layers which were smooth after deposition (figure 1a)), becomes now rough as the oxidation temperature increases (see insert in figure 4 for Film *3*) being this effect more patent on both Film *2* and *3*. These morphological discrepancies could correspond to some recrystallization process of the sp^2 clusters. Coatings having a quite high atomic surface roughness will be easily etched away on the clusters edges by H or O atoms. In opposition, homogeneous smooth more diamond-like coatings or surfaces of dense planes of graphite will present much lower oxidation rates. This is because the C-H and C-O bonds have energies of ~ 4.3 and ~ 3.8 eV [23], respectively, while C-C bonds can present much more different bonding values ranging from 7 down to < 1 eV [23]. Thus, it could be suggested that the oxidation behaviour will be dependent on the graphitic state developed by thermal effect on the non-oxidised a-C:H external layer.

3.2.2. Protective Environment

Following the same procedure used in oxidation tests, all films were analyzed in a mixture of Ar-5% H_2 atmosphere in order to study the single-handedly thermal effect. Figure 5a) presents the DSC/TG curves obtained for Film *3* in continuous heating of 40 ºC min^{-1} up to 800 ºC. The weight loss evaluated in the protective atmosphere is almost insignificant, ≅ 5 %, in opposition to that observed in oxidative environment, ≅ 90 % (see figure 2a) for the same coating). The weight does not decrease monotonously and two distinct trends can be associated with the simultaneous DSC/TG signals. For the first endothermic peak, with an onset temperature about 280 ºC, the TG curve slope is rather low and increases when the second endothermic reaction begins near 500 ºC.

Thus, isothermal TG tests were performed at the three typical temperatures involving DSC peaks: 250, 400 and 600 ºC (see figure 5b) for Film *3*). Besides the small shift for negative values of the starting isothermal points at 400 and 600 ºC, only a slight decrease of the weight is detected at 600 ºC, while no significant variations are registered after annealing during 60 min to temperatures of 250 and 400 ºC. Similar behaviour was obtained for samples *1* and *2*, indicating that coatings thickness was maintained without significant variation during annealing in protective environment up to 600 ºC.

Based on other thermal stability studies of hydrogenated carbon films [4, 6], the actual relationship between heat flux and weight variation can be identified as a thermal desorption process: the molecular hydrogen (H_2) evolution, above 250 ºC, precedes alongside with the formation of hydrocarbon molecules (C_xH_y) which occur near 500 ºC (see more details below). Both of these gases effusions are endothermic [4] in good agreement with the convexity of the DSC curves obtained in this study. Therefore, the two parts of the weight decrease of the TG curve in figure 5a) can be attributed to each one of those reactions, the first being less steep than the second, since H_2 molecules are much lighter than C_xH_y ones.

The hydrocarbon liberation is also a common situation reported by some authors during the film formation [2]. Indeed, a-C:H films are usually deposited at low temperatures in order to avoid this phenomenon and thus the deterioration of films properties. In order to shed some light on the structural evolution of the DLC films a series of Raman spectra was collected after isothermal annealing as shown in figure 6a) for the particular case of Film *1*. It is clear from these figures that below 400 ºC the only observable changes in the Raman spectra evolution is a small increase in the peak frequency of the a-C:H bands without changes its shape. This small shift tends to be regular with temperature and it has been detected in other works [3] being of no sufficient magnitude to clear indicate some important changes on the coatings structure. In fact, the integrated intensity ratio of D and G bands (I_D/I_G), derived from curve fitting and plotted in figure 6b), is similar to that obtained in the as-deposited state for all coatings and become only distinct for heat treatments above 250 ºC. At 400 ºC, the higher importance of the D-band, near 1350 cm^{-1}, coincides with the beginning of the G-band shift to higher wavelengths. Finally, at 600 ºC a substantive structural

change becomes apparent with the clear separation between the D and G bands, revealing that the coatings have developed the characteristics of the graphite-like regime. Thus, an increase of either the graphic rings or the number of graphitic sp^2 clusters can be expected similar to that observed in other research studies [4, 8, 10]. The considerable increase in I_D/I_G ratio from $\cong$ 1 (at RT) to $\cong$ 3.0 (at 600 ºC), figure 6b), envisage a strong softening of the coatings after thermal annealing. This can be confirmed in figure 7 presenting the evolution of the hardness after isothermal treatment in non-oxidative ambiance. The inset evolution in figure 7 shows that there is a good correlation between the hardness and the I_D/I_G ratio after thermal annealing, confirming the above analysis. At 600 ºC the hardness drops of about 60 % in relation to the post-deposition value (~ 20 to 12 GPa). However, it should be remarked that up to 400 ºC the hardness values only experimented a slight decrease in all the three studied coatings.

An overall discussion of the aforementioned results regarding the thermal behaviour of a-C:H coatings permits to conclude that below 400 ºC only desorption of hydrogen took place, which is reported in literature to occur near 300 ºC [3, 12]. This value is in good accordance with the first onset temperature DSC signal obtained in protective ambiance (figure 5a)). Nevertheless, the changes in both I_D/I_G ratio and G band frequency of the Raman spectra, from RT to 400 ºC (figure 6b)), confirm that graphitization process is become noticeable. The important structural changes due to H_2 effusion, such as the conversion of a part of the sp^3 sites into sp^2 sites, enhancement of sp^2 cluster size and the reduction of the stress and disorder [3, 23, 24] seems to be in contradiction with the hardness values obtained for the post-annealed films at 400 ºC (figure 7). The statements point out by Neuville *et. al* [23] in a relatively recent review work will be helpful to clarify this apparently opposition. It is reported that the presence of sp^3 sites is not the only criterion for diamond-like properties and the differences between the different possible binding energies in DLC-type coatings correspond to the distribution of C-sp^3 and C-sp^2 sites must also be considered [23]. Moreover, for hydrogenated coatings besides Csp^2-Csp^2 (~ 7.03 eV) and Csp^3-Csp^3 (7.02 eV) domains also the covalent bonds terminated by H atoms, H-Csp^1 (5.4 eV), H-Csp^2 (4.5 eV) and H-Csp^3 (4.1 eV) (usually denoted as C-H bonds of average energy of 4.3 eV) have to be take into account [23].

During the dehydrogenation reaction the recombination of H atoms to form gaseous H_2 will release chemical energy, considering the high binding energy of H-H (~ 5 eV) in comparison to C-H binding energy (~ 4.3 eV [23]), and thus the exo-diffusion of H_2 molecules take place alongside to the transformation of sp^3 to sp^2 sites [3]. But these thermodynamic considerations do not correspond to the observed endothermic DSC reaction. However it is also necessary to consider the higher binding energies of both Csp^2-Csp^2 in the sp^2 rings are getting larger during graphitization process (~7.03 eV [23]) and some possible atomic rearrangement in Csp^3-Csp^3 bonds (~ 7.02 eV [23]) corresponding to the reaction (3) proposed by Akkerman *et al.* [4].

$$2C(sp^3) - H \Rightarrow C(sp^3) - C(sp^3) + H_2 \qquad (3)$$
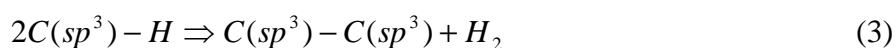
All these complex effects are balanced and mutually compensated and as a consequence, no significant hardness decrease should be expected as it was in fact observed up to 400 ºC. In opposition, at higher protective annealing temperatures (> 400 ºC), the continue effusion of the gaseous products, particularly in C_xH_y form, which match with the second DSC/TG signal, will occur. The gas liberation, results in the collapse of the carbon matrix, i.e. the sp^2 clusters combine and grow rapidly, in addition to an significant reduction of the stress and disorder and thus to the severe hardness decline.

The onset temperature for the thermal graphitization (figure 5a)) is almost coincident with the one of the thermal oxidation (figure 2a)), that is $\cong$ 500 ºC. This behaviour could be explained considering that oxygen can easily combine with reminiscent bonded H present in a-C:H films, due to the higher binding energy of O-H (4.8 eV) than C-O (3.8 eV), a reaction that transforms sp^3 sites to sp^2 and burns the graphitised carbon material. This is in accordance with the aforesaid experimental data revealing that low H-content films present the best oxidation resistance. Since oxidation reaction products are gaseous compounds any modified external passive layer in the a-C:H coatings is not formed. This is confirmed by the Raman spectra shown in figure 6a) for Film *1*, where the comparison between oxidative and protective annealed samples is presented. No differences in the spectra can be detected, presenting only the thermal effect in both samples.

4. Conclusions

Hydrogenated amorphous carbon thin films containing 25 to 29 at.% H were successfully deposited by PACVD. Their thermal stability, investigated up to 600ºC in different ambiances, put in evidence three of the most thermal harmful processes: dehydrogenation, graphitization and oxidation.

In protective atmosphere, two distinct thermal behaviours were detected. The first, for temperature up to 500ºC, the films were structurally stable maintaining their mechanical properties in the diamond-like regime (Hv ~20 GPa) in spite of the well detected dehydrogenation process; the second, achieved for higher annealing temperatures, leaded to the graphitization process in addition to gases effusion. At this point a substantive structural change was evident and the hardness values dropped to the graphite-like regime (Hv~12 GPa).

The heat treatments in air allowed correlate the thermal graphitization with thermal oxidation, being the onset temperature for both process almost coincident (~ 500 ºC). The damaging effect of oxidative annealing leading to a drastic decrease of the coatings thickness was more evident on higher H-content ones. Nevertheless, the coatings arquitecture developed by NA Bekaert by PACVD, seems to be an effective way for oxidation protection of the metallic substrate avoid the oxygen inward while maintain practical adhesion.

Finally it is important to mentioned that much more performing DLC of ta-C types exists, overcome some drawbacks of more usual DLC coatings of a-C:H type for many more demanding applications. However, for these achievements, they still need often to be better understood in many of their properties and coatings devices fundamentals and for which this study might play a part.

Research Highlights:

- A new coating design, through a a-C:H cap layer on a functional gradient film was successfully deposited by PACVD.

- The stability, functionality and long-term performance were evaluated in protective and oxidative ambiances.

- Up to 600 ℃ three thermal harmful processes were detected: dehydrogenation, graphitization and oxidation.

- The work describes the complex atomic rearrangements during annealing, function of temperature and composition, leading to important structural modifications.

- Coatings delamination and/or substrate oxidation were never detected.

References

[1] A.C. Ferrari, J. Robertson, Phys. Rev. B 61(2000) 14095.

[2] J. Robertson, Materials Science Engineering R: Reports 37 (2002) 129.

[3] D.R. Tallant, J.E. Parmeter, M.P. Siegal, R.L. Simpson, Diamond and Related Materials 4

(1995) 191.

[4] Z.L. Akkerman, H. Efstahiiadis, F.W. Smith, J. Appl. Phys. 80 (5) (1996) 3068.

[5] Q. Zhang, S.F. Yoon, Rusli, H. Yang, J. Ahn, J. Appl. Phys. 83 (3) (1998) 1349.

[6] J. Ristein, R.T. Stief, L. Ley, W. Beyer, J Appl. Phys. 84 (7) (1998) 38.

[7] R. Wachter, A. Cordery, Diamond and Related Materials 8 (1999) 504.

[8] A.A. Ogwu, R.W. Lamberton, S. Morley, P. Maguire, J. McLaughlin, P. Maguire, J.

McLaughlin, Physic B 269 (1999) 335.

[9] Won Jae Yang, Yong-Ho Choa, Tohru Sekino, Kwang Bo Shim, Koichi Niihara, Keun Ho Auh,

Thin Solid Films 434 (2003) 49.

[10] Z. Di, A.Huang, R.K.Y. Fu, P.K. Chu, L. Shao, T.Hochbauer, M. Nastasi, M. Zhang, W. Liu,

Q. Shen, S. Luo, Z. Song, C. Lin, J. Appl. Phys. 98 (2005) 053501-1.

[11] Hongxuan Li, Tao Xu, Chengbing Wong, Jianmin Chen, Huidi Zhou, Huiwen Liu, Thin Solid

Films 515 (2006) 2153.

[12] Ch. Wild, P. Koidl, Appl. Phys.Lett. 51 (19) (1987) 1506.

[13] X. Jiang, W. Beyer, K. Reichelt, J Appl. Phys. 68 (3) (1990) 1378.

[14] W.J. Wang, T.M. Wang, B.L. Chen, Nucl. Instr. and Meth. in Phys. Res. B 17 (1996) 140.

[15] J. -W. Jacquet, F. G. Wietig, Patent number: WO 2006/125683, 30 November 2006.

[16] J.M. Antunes, A. Cavaleiro, L.F. Menezes, M.I. Simões, J.V. Fernandes, Surf. Coat. Technol. 149 (2002) 27.

[17] C. Donnet, J. Fontaine, F. Lefebvre, A. Grill, V. Patel, C. Jahnes, J. Appl. Phys. 1999, 85(6), 3264.

[18] A. Singha, A. Ghosh, A. Roy, N.R. Ray, J. Appl. Phys. 100 (2006) 044910-1.

[19] J. Robertson, Diamond and Related Materials 1 (1992) 397.

[20] J. Robertson, Material Research Society Symposium Proceedings 555 (1999) 12.

[21] D-Y. Wang, C-L. Chang, W-Y. Ho, Surf. Coat. Technol. 120/121 (1999) 138.

[22] S. Zhang, X.L. Bui, X. Li, Diamond and Related Materials 15 (2006) 972.

[23] S. Neuville, A. Mattews, Thin Solid Films, 515 (2007) 6619.

[24]] J. Robertson, Diamond and Related Materials 3 (1994) 361.

Table 1. Main characteristics of the as-deposited DLC-based coatings.

Table 1

Characteristics	Film *1*	Film *2*	Film *3*	Remarks
H content (at. %)	25	27	29	External a-C:H layer
Ar content (at. %)	1.2	0.4	-	External a-C:H layer
Thickness (nm)	3000	1800	2400	External a-C:H layer
Thickness (nm)	4430	2580	3130	Total thickness
I_D/I_G	1.16	1.01	0.97	Raman D/G band ratio
Peak position (cm^{-1})	1559.9	1560.2	1557.4	Raman G band
Hardness (GPa)	19 ± 1.0	20 ± 0.4	21 ± 1.2	Ultramicroindentation
E-modulus (GPa)	158 ± 5.0	153 ± 7.5	174 ± 5.6	Ultramicroindentation
Roughness, Ra (μm)	0.007	0.008	0.007	AFM
Morphology	featureless and very smooth			SEM

Figure 1. a) ERD elemental composition of the as-deposited Film *1* and cross-section morphology of the as-deposited Film *2*; b) Raman spectra of the as-deposited a-C:H coatings (inset the example of the fitting procedure with four Gaussians for Film *3*).
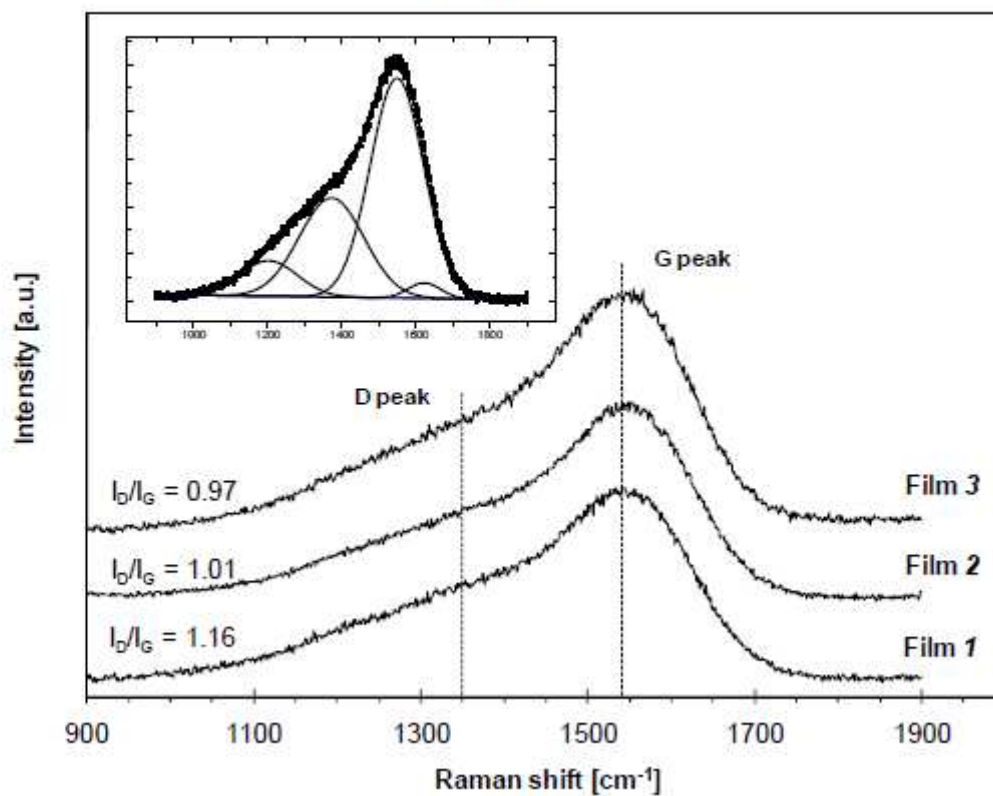
Figure 1 a)
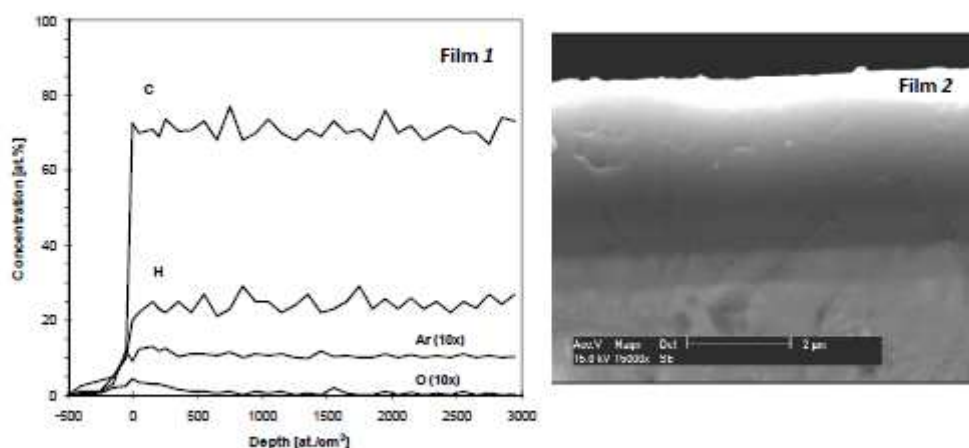
Figure 1 b)

Figure 2. Thermal analysis curves of the a-C:H coatings annealed in air; a) continuous DSC/TG heating; b), c) and d) isothermal TG heating.
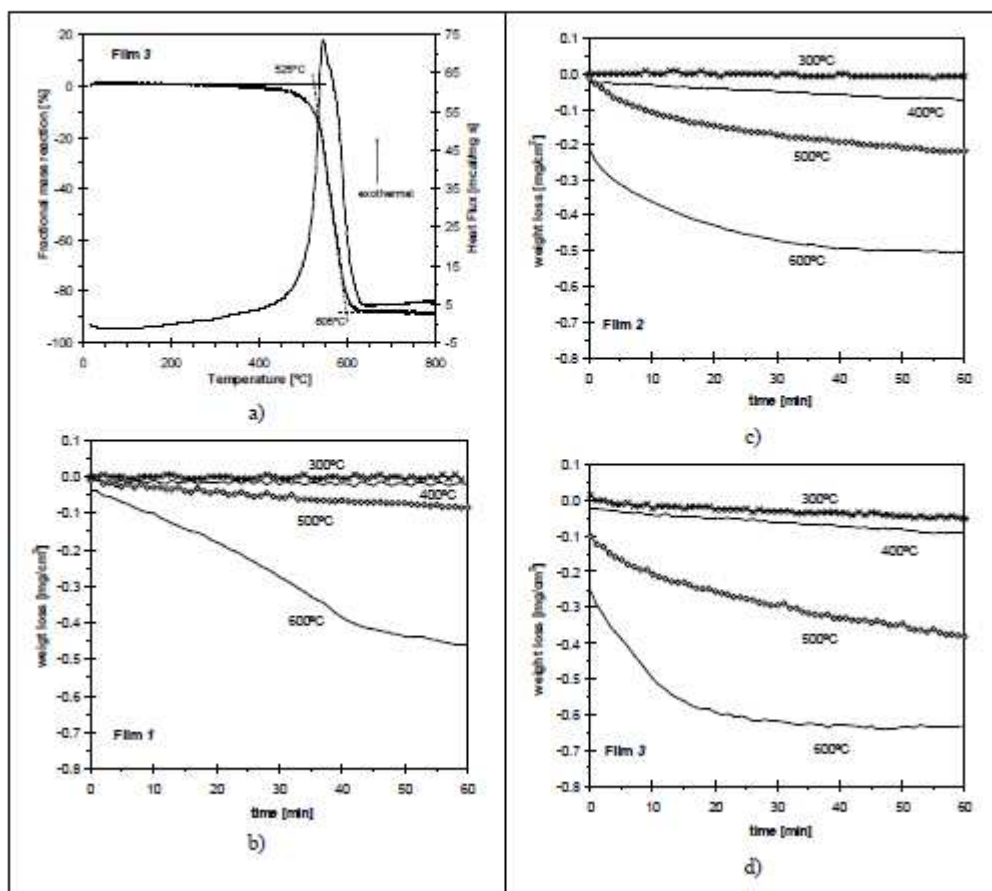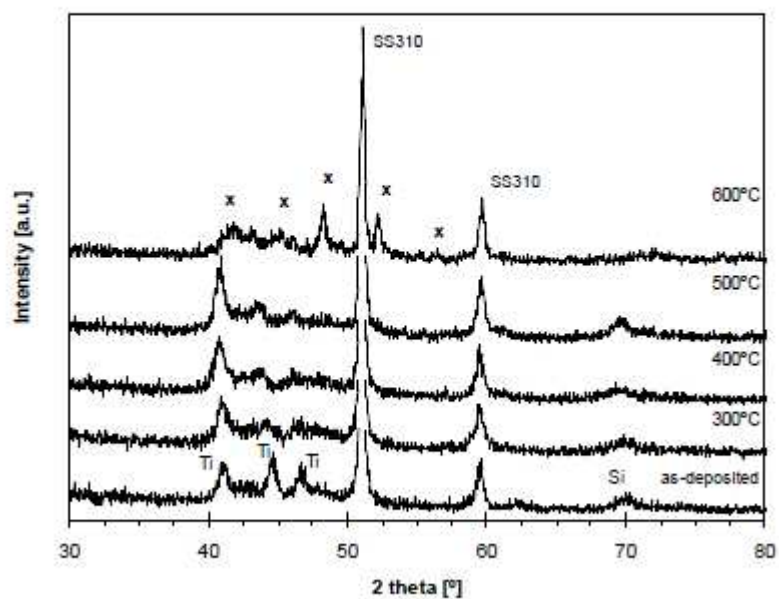
Figure 2

Figure 3. XRD structural evolution of Film *3* as a function of the oxidation temperature, x = TiC [ICDD 74-1219] or SiC [ICDD 31-1231] or Ti_5Si_3 [ICDD 78-1429].
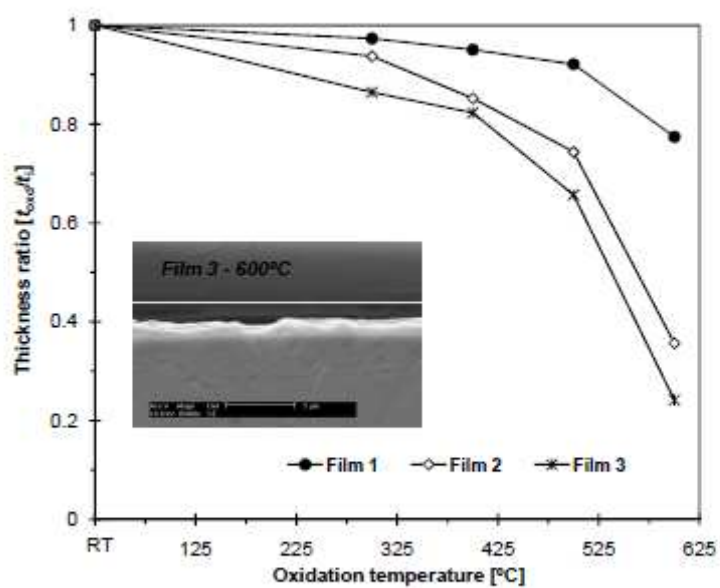
Figure 3

Figure 4. Normalized thickness variation of the external a-C:H layers after heating in air ambiance at different temperatures during 60 min (inset the cross-section morphology of the post-annealed Film *3* at 600 ℃).

Figure 4

Figure 5. Thermal analytical curves of the Film *3* in protective environment; a) continuous DSC/TG heating; b) isothermal TG heating.

Figure 5
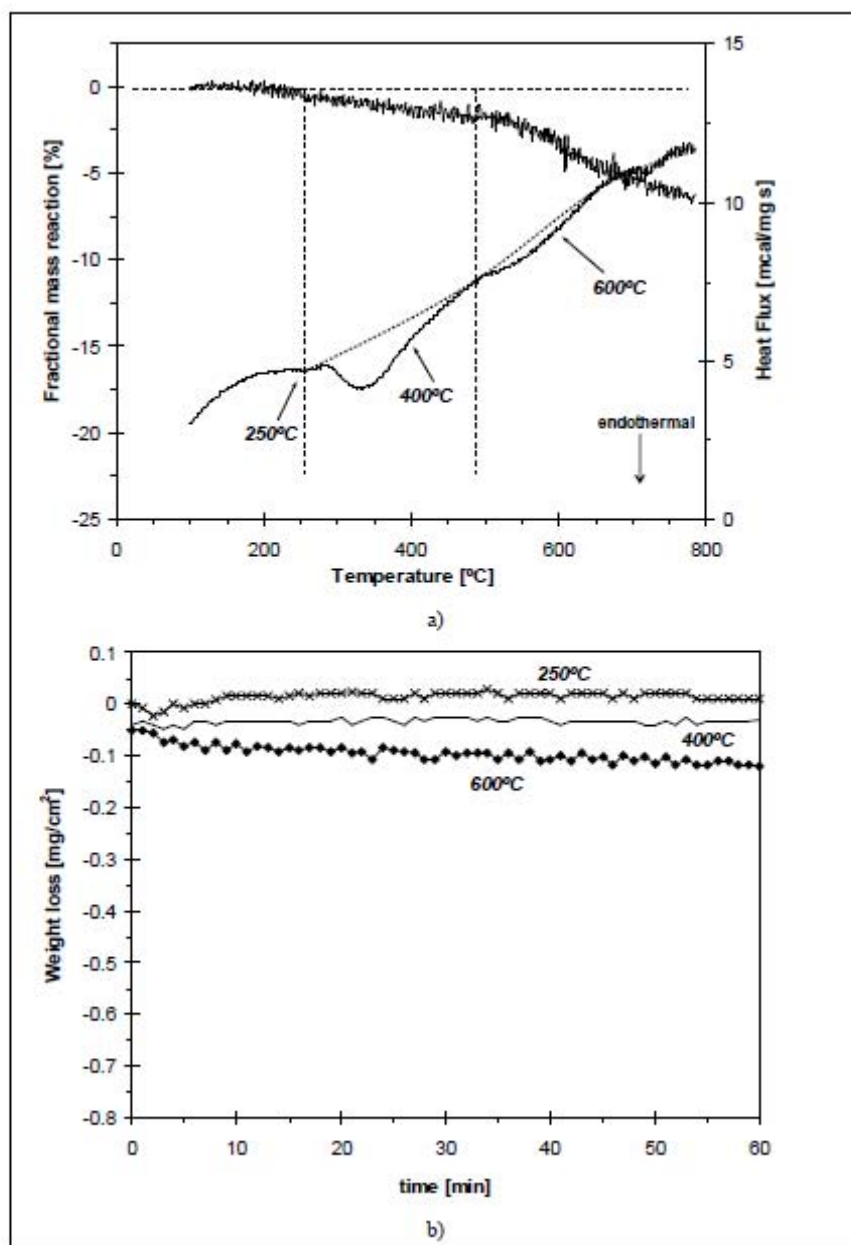
Figure 6. a) Evolution of the Raman spectra of a-C:H coatings as a function of the annealing temperature in both protective and oxidative atmosphere; b) I_D/I_G ratio and G band position derived from the Raman spectra curve fitting.
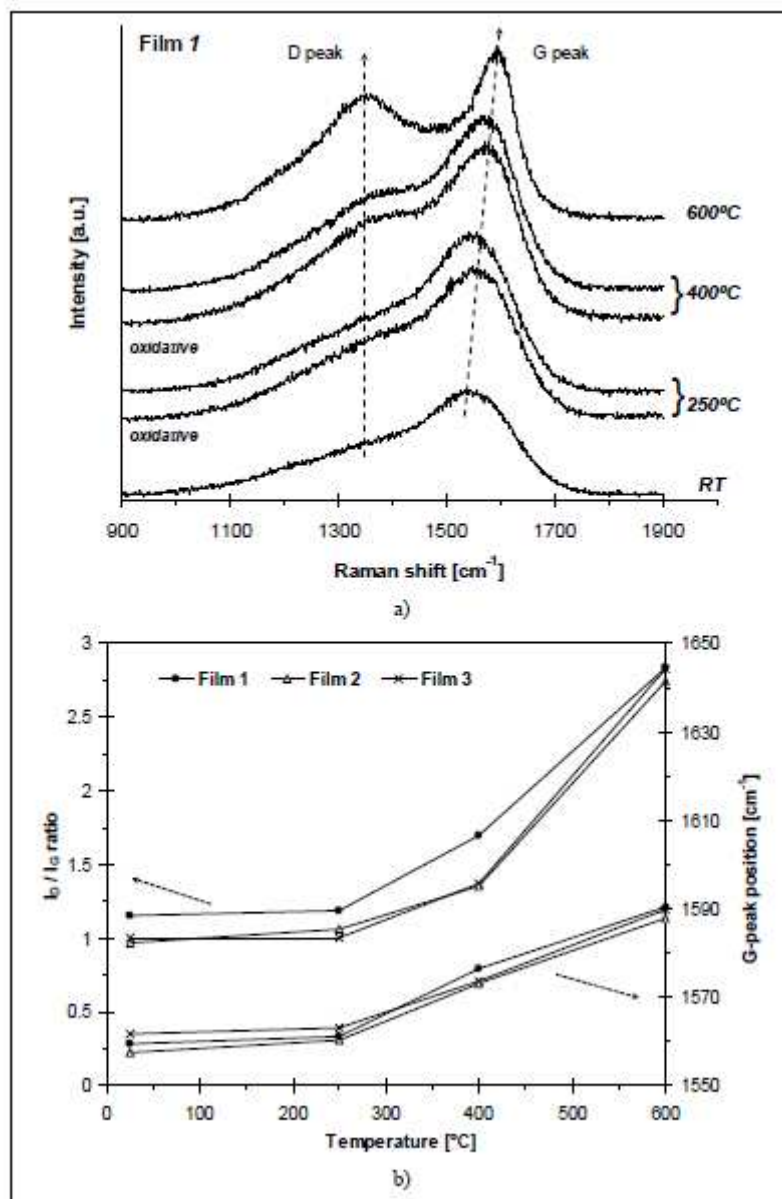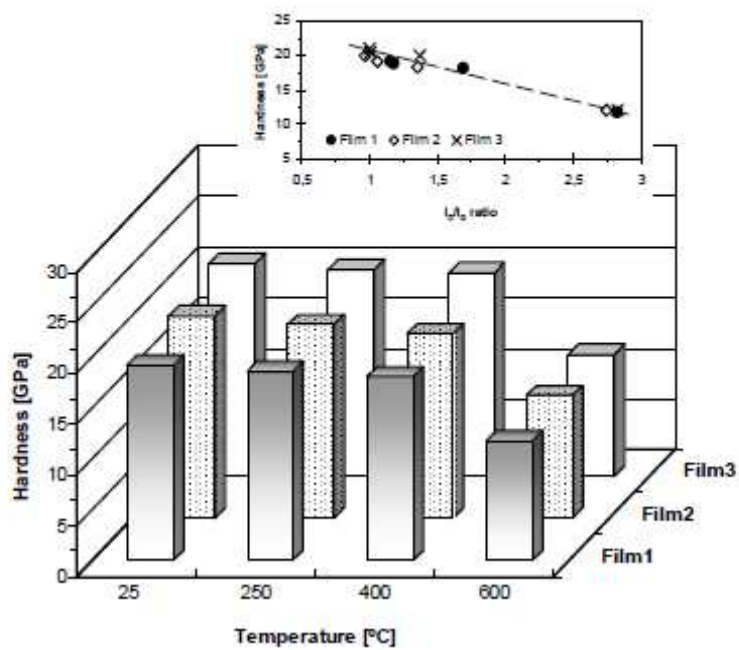
Figure 6

Figure 7. Hardness evolution of the a-C:H coatings as a function of the annealing temperature in protective atmosphere; inset of hardness versus I_D/I_G ratio (the dotted line is only a guide for the eyes).

Figure 7